

Investigation of the influence of the operating parameters on the magnetic encoder geometric error compensation.

Halil Ibrahim Cakar ¹, Ilyes Khelf ², Hugo André ¹

¹ Univ Lyon, IUT de Roanne, LASPI, 42334 Roanne Cedex, France

² ENGIE GREEN, 92400, Courbevoie, France
{hugo.andre}@univ-st-etienne.fr

Abstract

The encoder is the only sensor needed to perform Instantaneous angular speed (IAS) analysis, an alternative technique used to monitor gears, bearings or other electro-mechanical elements. The encoder is subject to an intrinsic defect called Geometric Error (GE). Although it has various origins, GE can be simplified as being related to the variable angular size of every encoder segments forming the theoretically uniform pattern. As a result, GE introduces a cyclic perturbation observed on the spectrum of the estimated IAS. These perturbations exhibit a first order cyclostationary behaviour which replicates themselves in each revolution of the shaft. Since the impacted frequency channels can also be studied to monitor the health status of the shaft line, GE should be corrected for a better IAS estimation.

In this study, a rotation domain averaging based algorithm is developed to compensate the GE of the estimated IAS signals. The GE signature of a given signal is estimated and is used to compensate the GE of the other signals as well as itself. The term cross-correction is introduced to mention the correction of signals with each other's GE signature. The quality of the correction is analysed and is shown that it depends on several operating conditions. In other words, signals obtained for certain operating conditions are shown to be better at correcting GE than signals obtained for different operating conditions.

The developed algorithm is tested on a 2-MW wind turbine campaign which is instrumented with a magnetic encoder. These observations makes it possible to qualify the properties of the best GE corrector signals and dress an optimized correction algorithm suitable for any database. Since there were several interventions on the wind-turbine like re-installation of the encoder, gearbox change and gear defect, it is also possible to observe the influences of these interventions on the GE compensation. The results of this work are expected to be useful for gearbox operators as it represents a probable solution for early fault detection especially in demanding operating conditions.

1 Introduction

In the specific domain of varying speed rotating machine diagnosis, Instantaneous Angular Speed (IAS) monitoring is one of the very interesting alternative to classical vibration measurement system. It has been tried to detect chatter in milling [2], bearing defects on wind turbines [3] or on truck wheels [1]... This technology first presents the advantage to be easy to install, since only one encoder is sensible to speed variations induced by components installed far away from it: in [4], the encoder installed on the high speed shaft of a turbine was shown able to monitor the low speed shaft characteristic frequencies, beyond the mechanical coupling and the three stage gear box. Moreover, the elapse time acquisition technique present the benefit to be intrinsically made in the angular domain, and therefore easily deal with macroscopic speed variations. However, this technique does not benefit from the same feedback than classical vibration monitoring, and plenty of questions need to be tackled before it can compete with it on an industrial scale. It has been shown able to detect different kinds of bearing problems, and mechanical models have been built up to justify the small speed variations induced by such defects [6]. The peculiar quantification error, specifically linked to the elapse time technique, along with the inability of IAS monitoring to be protected from aliasing phenomenon has been thoroughly studied in [7] and [8]. Geometric Error (GE) is another major limitation for IAS, since it is present on both acquisition techniques (ADC based and Elapse Time). This error is linked to several aspects: imperfection of the encoder

gratings, the interpolation process improperly tuned, or even the imprecise installation of the encoder. The common feature of all these aspects is their cyclic signature. Leclere et al proposed a technique to extract the GE from the IAS signal using rotation domain averaging [8], based on rotation domain averaging and used for steady speed signals. Bruand proposed two extra methods to adapt the GE estimation and correction to varying speed scenario [9]. The first is a data-driven approach based on a local weighted least squares method, while the latter is a model-based approach. The main drawback of all these approaches is linked to the fact that it is yet impossible to distinguish the GE from actual speed variations whose frequency is synchronous with the GE. In other words, if unbalance or gear mesh frequency happen to be coincident with the GE, they might disappear along with GE. This is troublesome if one is aiming at monitoring the unbalance of the gear-mesh health status. This paper comes within the scope of monitoring a defect whose frequency is synchronous with the shaft carrying the encoder. The main idea is to correct every measurement using the GE estimated using always the same signal, and to assume that the GE will not change from one measurement to the next. An evolution of the synchronous content would therefore be considered as actual speed variation, and therefore be assigned to the monitored element.

This paper aims at designing which signal(s) should be used to correct all consecutive measurement: to find the measurement that will rule the all... or to find the operating conditions that has an influence over the GE.

In order to avoid any terminological conflict, the measurement whose GE is used to correct all the measurements is called as the *Corrector Signal*. When one of the measurement is selected as the corrector signal, the other measurements are named as the *Signal to be Corrected*. When a measurement is corrected with the GE signature of the corrector signal, this measurement is called as the *Corrected Signal*. This terminology will be used throughout this manuscript. In the subsequent chapters the details are presented.

In the first part, the paper presents the method employed to estimate, to correct, and then to designate the what signals should be used to correct every others. The results obtained using a magnetic encoder on a long term measurement campaign are presented in the second part.

2 Method

This section first explains how is estimated the GE of an encoder using an elapse time measurement. Then, the correction process used on the corrected signal is presented. In the 3rd section, a quality indicator is presented to assess the quality of the processed corrected signal using the corrector signal. Finally, the maps used to synthesise the results will be introduced to efficiently show the influence of the operating conditions on the GE correction.

2.1 Geometric Error assessment

In the first step the GE signatures of both *Corrector Signal* and *Corrected Signal* are estimated. The method used in this paper is based on the one proposed by Leclere et al and quickly adapted to deal with non stationary speed [8]. Let first introduce the Rotation Domain Averaging (RDA) applied directly on the Elapse Time signal $\tau[j], j \in [1 : N \cdot R]$ with R the resolution of the encoder, N the number of revolution in the measurement. The RDA result is defined on one revolution: $\overline{\tau}[j], j \in [1 : R]$, such as:

$$\overline{\tau}[j] = \frac{1}{N} \sum_{k=1}^N \tau[j + k \cdot R] \quad (1)$$

Let then assume that the resulting RDA $\overline{\tau}[j]$ is only due to the GE on one hand, and to the macroscopic speed trend on the other hand. The latter is deduced from the original measurement with any kind of Low pass Filter (LF), whose cut-off frequency is lower than 1 per revolution. The RDA of the macroscopic trend is noted $\overline{\omega}_{LF}(j), j \in [1 : R]$. Then, the GE can be deduced from:

$$\overline{\tau}[j] = \frac{\Delta\theta}{\overline{\omega}_{LF}[j]} \rightarrow \Delta\theta[j] = \overline{\omega}_{LF}[j] \cdot \overline{\tau}[j] \quad (2)$$

In the special but ordinary case where the speed trend is steady once it is observed on the RDA (see figure 1 the left bottom plot) which means the average speed trend is steady and that every originally speed variation

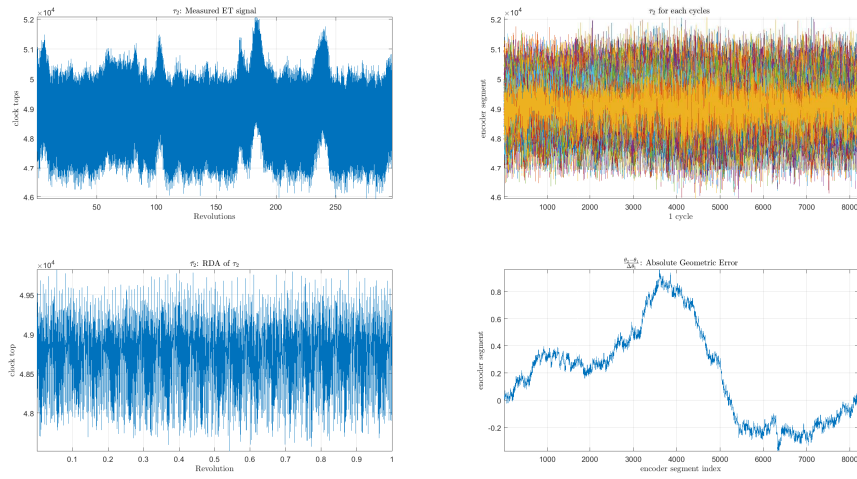


Figure 1 – GE Estimation of one of the measurements

rightfully compensates themselves, it is even possible to skip the low frequency filter and use the simplification proposed here under:

$$\Delta\theta[j] = \frac{\overline{\tau[j]}}{\sum_{i=1}^N \overline{\tau[i]}} \quad (3)$$

This steady speed assumption does not need the speed to be equal from one revolution to the next. However, it assumes that once the speed is averaged on every revolution, the resulting speed (1 revolution long) is steady. In the general case, and in this paper, the formulation proposed in Eq. 2 is preferred.

2.2 Cross Correction of the Geometric Error

The discrete integration of $\Delta\theta$ obtained in the previous section gives access to the angle θ between the launch of the counter clock and each consecutive encoder segment. These angles are not uniformly divided (that's the main reason of the paper!) and therefore influence the observed elapse time. From now on, these irregularly sampled angles are noted $\theta_2, j \in [1 : N \cdot R]$. As already mentioned, these errors are expected not to change from one revolution to the other, and from one measurement to the other.

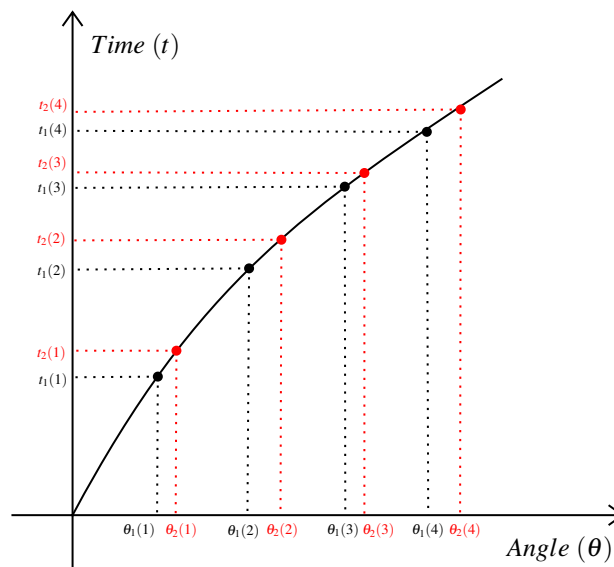


Figure 2 – Angle versus Time

The original elapse time measurement, obtained with irregularly sampled angles, are noted $t_2[j], j \in [1 : N \cdot R]$ once they are cumulated. A classical interpolation process is used to estimate the cumulated elapse time values $t_1[j], j \in [1 : N \cdot R]$ corresponding to the regularly sampled $\theta_1[j], j \in [1 : N \cdot R]$. In this section as in Fig. 2, presenting the correction process on a Time-Angle scheme, the index 2 stands for GE-Noised signal when the index 1 stands for the GE-corrected signal. the spline interpolation method has been chosen to estimate the GE-corrected values.

In this paper, one signal is used to correct an other. The *corrector signal* is used to obtain the angles $\theta_2[i] = \theta_2[j] + k \cdot N$. $\theta_1[i]$. The *signal to be corrected* is cumulated in $t_2[i] = \sum_{k=1}^i \tau_2[k]$, interpolated to give $t_1[i]$ and finally differentiated to estimate the elapse time we would get without GE: $\tau_1 i = t_1[i] - t_1[i-1], i \in [2 : N \cdot R]$. $\tau_1 i$ is the *corrected signal*.

2.3 Correction quality assessment

In order to asses the ability of one signal to accurately remove the GE from any other signal, the estimation of the GE removal quality is needed. The GE being concentrated on integer orders, due to its first order cyclostationary behaviour, the energy contained by the integer orders appears as the ideal indicator.

$$L_1 = \frac{1}{N} \sum_{m=1}^{N/2} \mathbf{F}_x^\theta(m) \quad (4)$$

with $\mathbf{F}_x^\theta(m)$ the DFT of the signal x computed for the order frequency m . This equation sums up the integer orders of the amplitude spectrum of the finite length signal. This corresponds to the sum of the TSA amplitude spectrum, and this is therefore not only representative of the GE, but also from every actual synchronous speed variations.

Fortunately, the order frequency of the most energetic synchronous speed variation are known. Unbalance and blade pass frequency is energetic up to the sixth order; gears frequencies are inducing energetic peaks on integer multiples of 93... Therefore we propose to remove these frequencies, and others, from the quality indicator. Equation 5 presents an example of such an indicator. More frequencies have been removed, but this paper will not bring out of the shadows these details for the sake of simplicity.

$$I = \frac{1}{N} \left(\sum_{m=1}^{N/2} \mathbf{F}_x^\theta(m) - \sum_{m=1}^9 \mathbf{F}_x^\theta(m) - \sum_{m=1}^{44} \mathbf{F}_x^\theta(93 \cdot m) \right) \quad (5)$$

2.4 Operating parameter analysis

This part presents the *cross-comparison* of several measurements obtained on one machine under various operating conditions, in order to investigate the quality of the correction process, and to designate the best operating to conditions to estimate GE. *Cross-comparison* is applied on a group of M measurement, where every measurement is used to successively correct every others. Once the *corrected signal* is corrected with the GE signature of the *corrector signal*, the GE correction efficiency is observed using the quality index presented in the previous section. Then, every measurement are arranged according to an operating parameter. For example, if the average power is the analysed operating parameter, the measurement are arranged in ascending order of mean power: the first signals are those acquired while the machine is not producing any current while the lasts were acquired at nominal power.

The result of the computation/arrangement is a matrix $I_{[M \times M]}$ which columns designate the *corrector signal* while its rows designate the *corrected signal*. Therefore, $I_{i,j}$ is presenting the quality index of the i^{th} measurement GE corrected using the j^{th} . Finally, Every rows are normalized with their corresponding *auto-corrected* values. Diagonal terms present the quality index obtained when the measurements are *auto-corrected*, ie they are corrected using their own GE estimation. Hence, the *cross-correction* matrices are obtained as in eq. 6.

$$I = \begin{pmatrix} 1 & \frac{I_{12}}{I_{11}} & \frac{I_{13}}{I_{11}} & \dots & \frac{I_{1m}}{I_{11}} \\ \frac{I_{21}}{I_{22}} & 1 & \frac{I_{2m}}{I_{22}} & \dots & \frac{I_{2m}}{I_{22}} \\ \dots & \dots & \dots & \dots & \dots \\ \frac{I_{m1}}{I_{mm}} & \frac{I_{m2}}{I_{mm}} & \frac{I_{m3}}{I_{mm}} & \dots & 1 \end{pmatrix} \quad (6)$$

The results presented hereafter will plot such cross correction matrices in greyscale colormaps. In this study, the number of measurements in each cross-comparison group is limited to $M = 300$ to save computation time.

3 Experimental results

3.1 Campaign presentation

A long term study is being carried over a MM92 wind turbine. The wind turbine set-up is presented in Figure 3 for the reader to realize the easiness of the involved instrumentation in regards with the kinematic complexity of the turbine line shafting. The speed transmission is made of one star epicyclic gear train and one parallel stage mounted in serial configuration to obtain a global speed ratio approximately equal to 119. The IAS signal can be computed from the generator optical encoder, which is the high quality incremental encoder used by the converter to correctly synchronize the asynchronous generator; but also from a lower quality magnetic encoder, installed in a retrofit operation on the low speed shaft directly carrying the rotor hub. It has been decided to equip the low speed shaft since the most expensive shaft line elements are kinematically and physically closer from it. This study will focus on this 20480 pulses per rev magnetic encoder installed beyond the slip ring, on the low speed shaft.

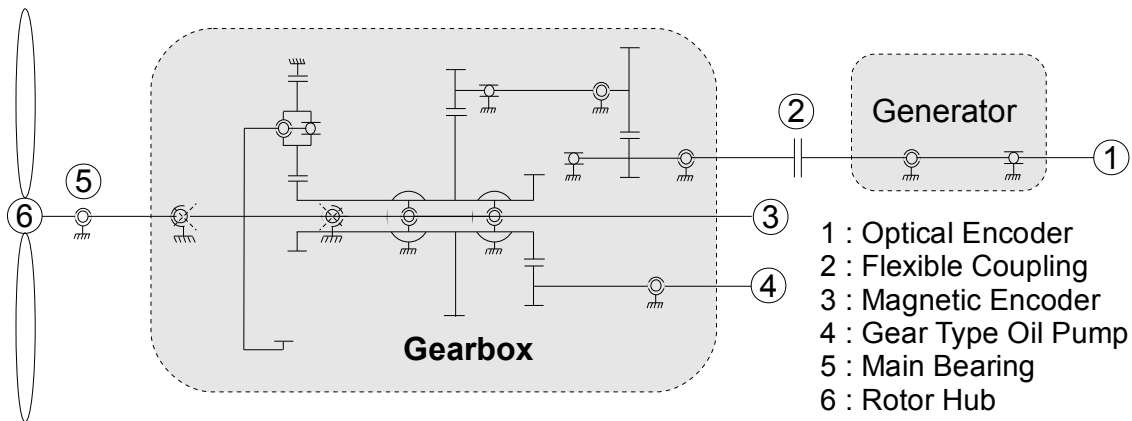


Figure 3 – Kinematic Scheme of the wind turbine set-up.

The measurement have been acquired between august 2017 and October 2018 on the same machine. Since the machine was suffering a major gear crack on the epicyclic ring, the gear box and the magnetic encoder were changed on the 25th of September. Nothing but the new gearbox running in was expected to be seen later on.

The acquisition card, FPGA type, is embedded in an industrial PC directly installed in the nacelle and reads the elapse time signal with a 120MHz counter clock. The signals are 300 revolutions long, and are synchronized with 1hz process data describing the operating conditions:

- date
- wind speed / direction,
- active/reactive/actual power,
- nacelle orientation,

- inside/outside temperature

All these operating parameters were analysed through the process detailed in the previous part. This paper will only present the most interesting results.

3.2 Resulting maps

This section successively presents the parameters that have been seen to play a role in the GE correction quality, starting from the most influential.

3.2.1 Influence of the Date

The 300 measurements on the cross-comparison map shown in Fig. 4 have been selected randomly before and after the encoder removal date. The only condition was set on the minimum gearbox speed, which must be greater than $800rpm$ to avoid start/stop measurement. Those measurement have been successively cross-corrected according to every available operating parameter. And the date criteria appeared as the the most informative one. The diagonal of the plot presents the lowest values: 1. This reminds that the auto-corrected values are used as references.

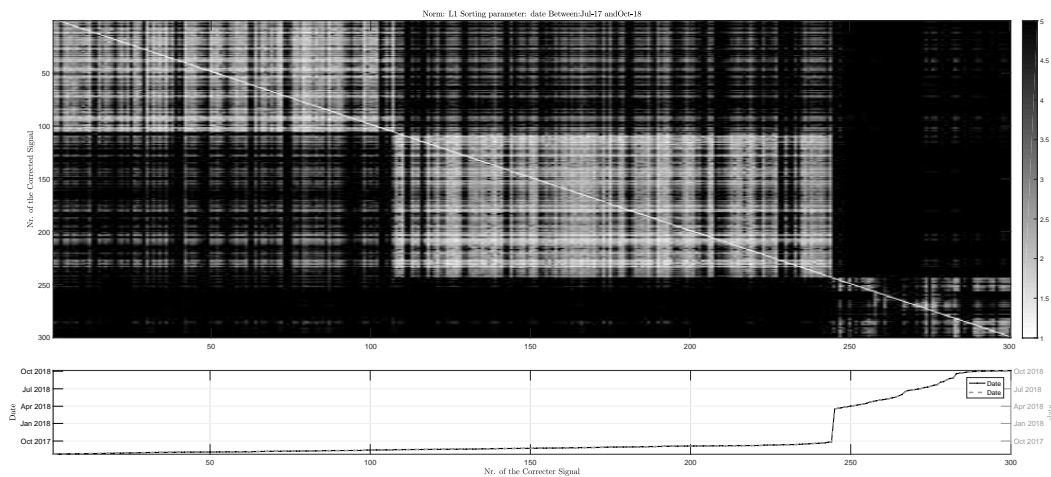


Figure 4 – Cross correction map sorted by date. The bottom plot reads the date of each measurement.

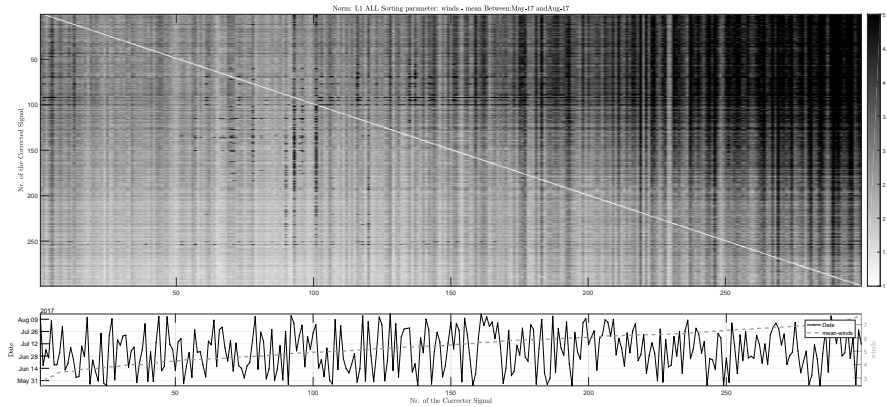
Unlike the maps obtained using other parameters, this map clearly exhibits vast light and dark regions. Lighter regions means every signal within it correct and are corrected in a better way between themselves. The top left region is limited by the measurement 105th, which has been acquired just before encoder removal, on 25th September, 2017. If the measurements obtained before this date are corrected by measurement obtained after: the quality of the correction is lower. This observaiton confirms that the removal of the encoder, the orientation and the geometric position between the encoder ring and the reader head modify the GE.

Moreover, still looking at figure 4, one may pay attention to the bottom right region, starting on the 244th measurement. There is no clear explanation to this sudden change of behaviour. The history of this machine was checked by its owners: it was noticed that there was only one distant reset on the machine but no encoder removal. A distant reset is the routine action performed remotely by the supervising operators when a minor alarm stops the machine. Such an alarm is sometimes reseted without further analysis if it does not repeat. This coincidence is interesting, though not demonstrative.

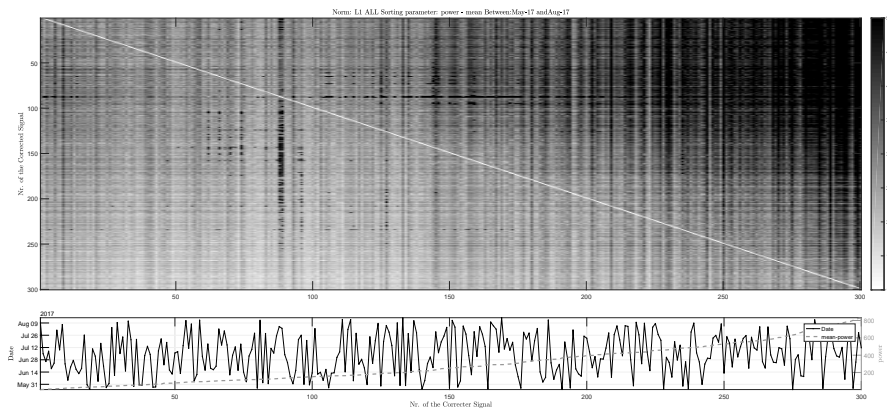
3.2.2 Influence of the Power and Wind Speed

Let’s now investigate the next most influential parameter. 300 new measurements are selected using the same conditions as before, plus a date criteria: measurement must be acquired between May and August (the

bottom right region observed in the previous section). Among the different re-sorted matrices, the matrices sorted according to their mean power and the mean wind speed were observed to be the best classifiers. The sorted maps demonstrate the similar behavior as observed on figure 5a and figure 5b, which is fairly normal: actual power and wind speed are linearly correlated.



(a) Mean Wind Speed



(b) Mean Power

Figure 5 – (a)Cross correction map sorted by wind speed. The bottom plot reads the date and the average wind speed of each measurement. (b) Cross correction map sorted by actual power. The bottom plot reads the date and the average actual power of each measurement.

3.2.3 Influence of the Nacelle

Let's now investigate the next most influential parameter. 300 new measurements are selected using the same conditions as before, plus a power criteria: measurement must be acquired between 0 and 300 watts. Among the different re-sorted matrices, the matrices sorted according to their mean nacelle direction were observed to be the best classifier. Figure 6 present an interesting *cross shape*, showing that low values are well corrected by low and by high nacelle direction values. Indeed, low and high nacelle direction values both correspond to the north direction, while 180 degrees correspond to the south direction. The most reasonable explanation is that the earth magnetic field influences the magnetic encoder GE. An alternative explanation was linked to the topographic environment of the turbine, but the monitored machine was actually shown to stand in the middle of a naked plain, far away from any forest, hills, or other turbine's wake effect.

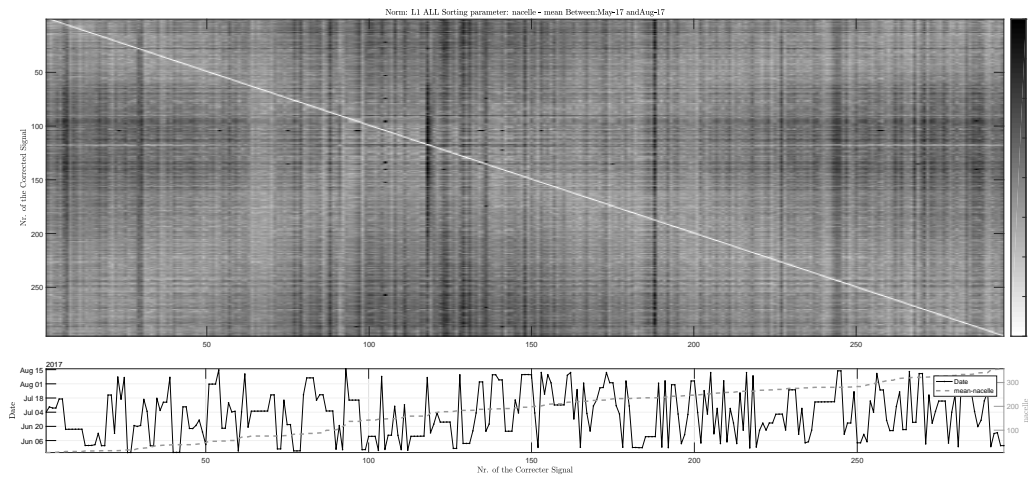


Figure 6 – Map demonstrates the influence of the nacelle values on GE correction efficiency. *The map is sorted by mean nacelle values.*

4 Conclusion and perspective

Instantaneous angular speed monitoring is often based on the use of an angular sensor, such as an encoder, whose gratings are often perturbed by an unequal distribution. This problem might be due to the manufacturing, the installation of even to the calibration of the electronics used to interpolate the signal. Anyhow, this kind of defect is called Geometric Error, and is interpreted as speed variations whose frequencies are the orders of the shaft carrying the encoder. Among the various techniques existing to remove GE, none spare the actual synchronous speed vibration. therefore, how to monitor a gear whose amplitude is biased by GE ? The solution proposed in this paper is to correct every signals GE obtained on a machine with one reference signal. if something evolves: it's the synchronous component! Finally, one signal is not yet enough to characterise the GE. low speed measurement appear as a good corrector, but the GE need to be reseted when the encoder ring or sensor is reinstalated. Moreover, the orientation of the sensor regarding the earth magnetic field has to be taken into account. The latest issue might be tackled by a model correcting the influence of the magnetic field on the sensor, knowing the orientation of the gratings during the reference and the corrected measurement.

4.1 Acknowledgements

the authors would like to thank ENGIE GREEN for their long term support. Instantaneous Angular Speed is a box full of both good surprises barriers to be broken down. For the latter, they indisputably deserve a good part of the merit.

References

- [1] L. Renaudin, F. Bonnardot, O. Musy, J.B. Doray, D. Rémond, Natural roller bearing fault detection by angular measurement of true instantaneous angular speed, *Mechanical Systems and Signal Processing*, Volume 24, Issue 7, October 2010, Pages 1998-2011, ISSN 0888-3270, <http://dx.doi.org/10.1016/j.ymsp.2010.05.005>
- [2] M. Lamraoui, M. Thomas, M. El Badaoui, F. Girardin, Indicators for monitoring chatter in milling based on instantaneous angular speeds, *Mechanical Systems and Signal Processing*, Volume 44, Issues 1-2, 2014, Pages 72-85, ISSN 0888-3270
- [3] H. André, A. Bourdon, D. Rémond, On the use of the Instantaneous Angular Speed measurement in non-stationary mechanism monitoring. *Proceedings of the ASME 2011 International Design Engineering Technical Conferences & 23rd Biennial Conference on Mechanical Vibration and Noise, IDETC/CIE 2011*, Washington, DC, USA

- [4] H. Andre, I. Khelf, Q. Leclere, Harmonic product spectrum revisited and adapted for rotating machine monitoring based on IAS., *Surveillance* 9, 2017, Fes, Morocco
- [5] C.J. Stander, P.S. Heyns, Instantaneous angular speed monitoring of gearboxes under non-cyclic stationary load conditions, *Mechanical Systems and Signal Processing*, Volume 19, Issue 4, 2005, Pages 817-835, ISSN 0888-3270
- [6] J.L. Gomez, A. Bourdon, H. André, Didier Rémond, Modelling deep groove ball bearing localized defects inducing instantaneous angular speed variations, *Tribology International*, Volume 98, 2016, pp 270-281
- [7] H. André, F. Girardin, A. Bourdon, J. Antoni, D. Rémond, Precision of the IAS monitoring system based on the elapsed time method in the spectral domain, *Mechanical Systems and Signal Processing*, Volume 44, Issues 1-2, 20 February 2014, Pages 14-30, ISSN 0888-3270, <http://dx.doi.org/10.1016/j.ymssp.2013.06.020>
- [8] Q. Leclere, F. Girardin, D. Rémond. An Analysis of Instantaneous Angular Speed Measurement Errors. *Surveillance 7 International Conference*, Oct 2013, CHARTRES, France. pp.1-11. hal-00905103
- [9] G. Bruand, F. Chatelain, P. Granjon, N. Martin, C. Duret, et al., Estimating the Rotational Synchronous Component from Instantaneous Angular Speed Signals in Variable Speed Conditions. *International Conference on Condition Monitoring of Machinery in Non-Stationary Operations (CMMN0'2018)*, Jun 2018, Santander, Spain. hal-01761532